Earth and Planetary Science Letters 270 (2008) 63–72

Contents lists available at ScienceDirect

Earth and Planetary Science Letters

journal homepage: www.elsevier.com/locate/epsl

Different isotope and chemical patterns of pyrite oxidation related to lag and exponential growth phases of *Acidithiobacillus ferrooxidans* reveal a microbial growth strategy

Benjamin Brunner [a,*], Jae-Young Yu [a,b], Randall E. Mielke [a], John A. MacAskill [c], Stojan Madzunkov [c], Terry J. McGenity [d], Max Coleman [a]

[a] Planetary Science and Life Detection Section, Jet Propulsion Laboratory, California Institute of Technology, 4800 Oak Grove Drive, Pasadena, CA 91109, USA
[b] Department of Geology, Kangwon National University, Chuncheon, Kangwon-Do 200-701, Republic of Korea
[c] Astrophysics and Space Sciences Section, Jet Propulsion Laboratory/Caltech, 4800 Oak Grove Drive, Pasadena, CA 91109, USA
[d] Department of Biological Sciences, University of Essex, Wivenhoe Park, Colchester, Essex, CO4 3SQ, UK

ARTICLE INFO

Article history:
Received 6 July 2007
Received in revised form 20 February 2008
Accepted 4 March 2008
Available online 18 March 2008

Editor: G.D. Price

Keywords:
Acidithiobacillus ferrooxidans
pyrite oxidation
growth phases
oxygen and sulfur isotope
composition of sulfate
degassing of sulfur dioxide from acid solutions
sulfite

ABSTRACT

The solution chemistry during the initial (slow increase of dissolved iron and sulfate) and main stage (rapid increase of dissolved iron and sulfate) of pyrite leaching by *Acidithiobacillus ferrooxidans* (*Af*) at a starting pH of 2.05 shows significant differences. During the initial stage, ferrous iron (Fe^{2+}) is the dominant iron species in solution and the molar ratio of produced sulfate (SO_4^{2-}) and total iron (Fe_{tot}) is 1.1, thus does not reflect the stoichiometry of pyrite (FeS_2). During the main stage, ferric iron (Fe^{3+}) is the dominant iron species in solution and the SO_4^{2-}:Fe_{tot} ratio is with 1.9, close to the stoichiometry of FeS_2. Another difference between initial and main stage is an initial trend to slightly higher pH values followed by a drop during the main stage to pH 1.84. These observations raise the question if there are different modes of bioleaching of pyrite, and if there are, what those modes imply in terms of leaching mechanisms.

Different oxygen and sulfur isotope trends of sulfate during the initial and main stages of pyrite oxidation confirm that there are two pyrite bioleaching modes. The biochemical reactions during initial stage are best explained by the net reaction $FeS_2 + 3O_2 \Rightarrow Fe^{2+} + SO_4^{2-} + SO_2(g)$. The degassing of sulfur dioxide (SO_2) acts as sink for sulfur depleted in ^{34}S compared to pyrite, and is the cause of the SO_4^{2-}:Fe_{tot} ratio of 1.1 and the near constant pH. During the exponential phase, pyrite sulfur is almost quantitatively converted to sulfate, according to the net reaction $FeS_2 + 15/4O_2 + 1/2H_2O \Rightarrow Fe^{3+} + 2SO_4^{2-} + H^+$. We hypothesize that the transition between the modes of bioleaching of pyrite is due to the impact of the accumulation of ferrous iron, which induces changes in the metabolic activity of *Af* and may act as an inhibitor for the oxidation of sulfur species. This transition defines a fundamental change in the growth strategy of *Af*. A mode, where bacteria gain energy by oxidation of elemental sulfur to sulfite but show little growth is switched into a mode, where bacteria gain a smaller amount of energy by the oxidation of ferrous iron, but induce much faster pyrite leaching rates due to the production of ferric iron.

1. Introduction

Bacteria are important mediators of geochemical reactions. Due to its contribution to acid mine drainage problems, the bacterial oxidation of pyrite by *Acidithiobacillus ferrooxidans* (*Af*) is one of the best-studied examples of such a process. Pyrite oxidation rates are dramatically increased by the role of *Af* in the oxidation of ferrous to ferric iron. While bacterial oxidation of ferrous iron has been studied intensely and is well understood, the initiation of pyrite leaching by *Af* has only been investigated in a few studies (e.g. Mustin et al.; 1992; Yu et al.; 2001; Mielke et al.; 2003) and characterization of the chemical reactions resulting in sulfur and oxygen isotope fractionations is lacking so far. A deeper understanding of the bacterial mechanisms in the initial stage of pyrite leaching is essential in terms of ecology and evolution of *Af* (survival strategies) and for the evaluation of isotope patterns related to oxidation of pyrite that could indicate presence or absence of life (biomarkers).

During the initial stage of pyrite oxidation in the presence of *Af*, iron is mostly accumulated in its ferrous form, Fe^{2+}, and the accumulation rates of iron and sulfate do not correspond to the 2:1 stoichiometry for sulfur and iron in pyrite (e.g. Mustin et al.; 1992; Yu et al.; 2001). In the main stage of pyrite leaching by *Af*, the leaching products are sulfate and ferric iron (Fe^{3+}), and their ratio is close to the 2:1 sulfur–iron stoichiometry of pyrite (FeS_2) (Yu et al.; 2001). The

* Corresponding author. Currently at Max-Planck-Institute for Marine Microbiology, Celsiusstrasse 1, Bremen 28359, Germany.
E-mail address: bbrunner@mpi-bremen.de (B. Brunner).

0012-821X/$ – see front matter © 2008 Elsevier B.V. All rights reserved.
doi:10.1016/j.epsl.2008.03.019

curious discrepancy in the solution chemistry between different stages of pyrite leaching by *Af* leads to the hypothesis that the pyrite oxidation mechanism in the presence of *Af* in the initial stage of pyrite oxidation is different from the one in the main stage.

1.1. The Yu et al. (2001) experiments

Yu et al. (2001) carried out batch pyrite leaching experiments with *Af* with open access to air in acidic conditions at a pH of 2.04 and they monitored the extent of evaporation of the media. They observed two stages of pyrite leaching, an initial stage where Fe^{2+} and sulfate were the main products, and after approximately 400 h, a second stage with Fe^{3+} and sulfate as main products (Fig. 1). In the initial stage, the production of dissolved iron and sulfate was generally low (2.5 mmol SO_4^{2-}/L, 1.7 mmol Fe^{2+}/L in 381 h), and decreased with time. However, compared to nonbiological (uninoculated) leaching of pyrite under the same conditions, *Af* considerably increases the leaching rate during the initial stage of pyrite leaching (Fig. 1). The second stage of pyrite leaching is marked by strongly increased production rates of iron and sulfate, and therefore, is called the main stage of pyrite leaching. During the initial phase of pyrite leaching, the number of bacteria stayed low and most of the bacteria were attached to the pyrite surface. At the end of the initial leaching stage there is a significant reduction in cell count. During the main stage of pyrite oxidation, the number of bacteria grew dramatically and most bacteria were detached from the pyrite surface (Fig. 1; Table 1).

The change between the modes of pyrite leaching is marked by a change in the ratio of produced sulfate to iron (Fig. 2). During the initial stage, the SO_4^{2-}/Fe_{tot} ratio was 1.1 ± 0.1, a behavior that has been called nonstoichiometric, referring to ratios that are not equal to the 2:1 stoichiometry of pyrite (FeS_2). During the main stage, the SO_4^{2-}/Fe_{tot} ratio was 1.9 ± 0.0, thus almost stoichiometric. This change is accompanied by a change in the pH of the solution: the pH of the solution stayed constant or slightly increased (2.08 ± 0.04) during the initial stage and dropped to pH 1.84 ± 0.04 in the main stage of pyrite leaching (Fig. 2).

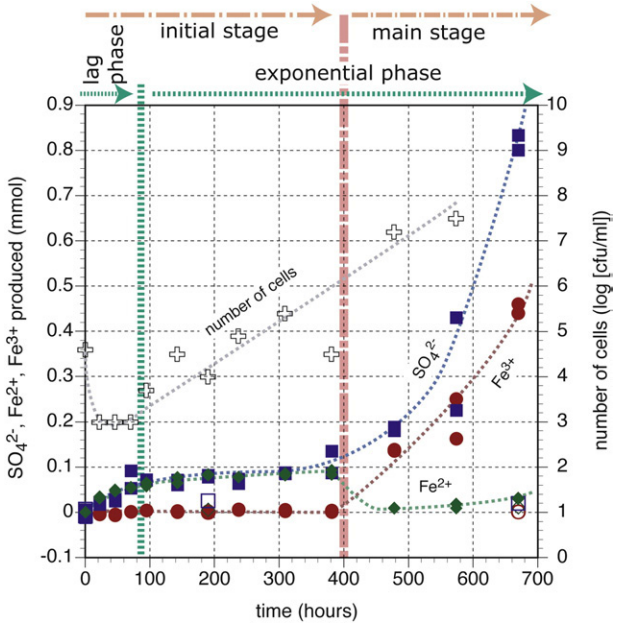

Fig. 1. The dotted lines highlight the trends in the amount of produced Fe^{2+}, Fe^{3+}, SO_4^{2-} and the number of cells. Interestingly, the production of sulfate and ferrous iron almost ceases between the start of the exponential phase of growth and the end of the initial stage of pyrite leaching. The dashed vertical lines mark the transition from lag phase to exponential phase of growth and initial stage to main stage of pyrite leaching. Symbols: crosses: number of cells; filled squares: produced sulfate (*Af*); hollow squares: produced sulfate (uninoculated); filled diamonds: produced Fe^{2+} (*Af*); hollow diamonds: produced Fe^{2+} (uninoculated); filled circles: produced Fe^{3+} (*Af*); hollow circles: produced Fe^{3+} (uninoculated).

The nonstoichiometric behavior of the SO_4^{2-}/Fe_{tot} ratio in the solution implies that not as much sulfur as iron is leached from pyrite as one would expect from strict dissolution of FeS_2, or that other sulfur species than sulfate (e.g. elemental sulfur S^0, sulfite SO_3^{2-}, thiosulfate $S_2O_3^{2-}$) are accumulated. Yu et al. (2001) neither detected any elemental sulfur by Soxhlet extraction (detection limit, 10 μmol), nor dissolved sulfur species besides sulfate by ICP-AES (detection limit, 1 ppm). We, therefore, refer to this undetected sulfur species as "missing sulfur". The SO_4^{2-}/Fe_{tot} ratio (Fig. 2) clearly shows that the "missing sulfur" was not converted to sulfate at the beginning of the main stage of pyrite leaching, but remained missing. As indicated by the SO_4^{2-}/Fe_{tot} ratio of 1.9 during the main stage, "sulfur loss" still continues.

1.2. Nonstoichiometric leaching of pyrite in abiotic experiments

Interestingly, nonstoichiometric leaching of pyrite has also been observed in abiotic experiments: Descostes et al. (2004) report SO_4^{2-}/Fe_{tot} ratios of 1.5 to 1.6 at pH of 1.2 to 2 in abiotic experiments with perchloric and hydrochloric acid and present a data compilation that indicates that the observed ratio depends on the pH of the solution. Descostes et al. (2004) suggest that the "missing sulfate" may have degassed as sulfur dioxide (SO_2).

1.3. Speciation of sulfite, and potential degassing of sulfur dioxide (SO_2)

Sulfite is an important intermediate in biologic oxidation of sulfur compounds (e.g. Vestal and Lundgren, 1971; Eccleston and Kelly, 1978; Pronk et al., 1990; Hirose et al., 1991; Suzuki et al., 1992; Wodara et al., 1997; Masau, 1999; Friedrich et al., 2001; Rohwerder and Sand, 2003; Wakai et al., 2004; Rawlings, 2005; Sugio et al., 2006) and likely to be an important intermediate in the pyrite leaching mechanism. In the absence of an oxidant (e.g. Fe^{3+}), it may accumulate in solution. At a pH of 2, speciation programs (such as visual MinteQ®), calculate that 37% of sulfite is present as H_2SO_3 (sulfurous acid molecule). However, there is no evidence for the existence of H_2SO_3 (Betts and Voss, 1970; Horner and Connick, 2003 and references therein), the most acidic species is sulfur dioxide (SO_2). Thus, 37% of the sulfite species in an acid solution must exist as volatile sulfur dioxide.

1.4. Observations from sulfur and oxygen isotope studies

The sulfur in sulfate of pyrite leaching solutions is ultimately derived from pyrite. If pyrite is quantitatively oxidized to sulfate, no sulfur isotope fractionation can occur and the sulfur isotope composition of sulfate reflects that of pyrite. However, if sulfur pools other than sulfate are formed, sulfur isotope fractionation can occur and the actual oxidation mechanism of pyrite sulfur becomes important. Sulfur isotope fractionation may occur during the stepwise oxidation of pyrite sulfur, when existing sulfur species are consumed (e.g. breaking of S–S bond when thiosulfate is transformed into elemental sulfur and sulfite) and new sulfur species are formed (e.g. oxidation of elemental sulfur to sulfite), or also when sulfur isotopes are exchanged (e.g. sulfur isotope exchange between sulfonate and sulfane sulfur of the thiosulfate molecule, Uyama et al., 1985; Chu et al., 2004). Thus, the sulfur isotope composition of sulfate from leaching of pyrite preserves information about the isotope composition of the leached pyrite, as well as information about potential diversion of sulfur species in pools other than sulfate. Commonly, sulfur isotope fractionation related to abiotic and biotic oxidation of sulfur species is relatively small (Taylor et al., 1984; Toran and Harris, 1989; Balci et al., 2007; Pisapia et al., 2007 and references therein).

Under neutral conditions (pH 7) and at ambient temperatures (25 °C), oxygen isotope exchange between sulfate and water is

Table 1
Solution chemistry and isotope composition of sulfate and water during acid leaching of pyrite

Pyrite leaching stage	*Af* growth phase	Time (h)	pH	Cell[a] count (cfu/ml)	SO_4[b] (total) (mmol)	SO_4[c] (pyrite) (mmol)	Fe (total) (mmol)	Fe(II) (mmol)	Fe(III) (mmol)	*X*[d]	H_2O δD	H_2O $\delta^{18}O$	SO_4 (total) $\delta^{34}S$	SO_4 (total) $\delta^{18}O$
Control		0.55	2.05	U	0.25	0.01	0.00	0.00	0.00	0.03	−41.5	−5.8	3.5	7.5
		0.62	2.03	U	0.24	−.01	0.00	0.00	0.00	−.03	−40.6	−3.3	3.5	7.7
		190.30	2.02	<10	0.27	0.03	0.01	0.01	0.00	0.09	−37.1	−3.8	3.4	6.5
		669.92	1.92	U	0.27	0.02	0.01	0.01	0.00	0.07	−26.4	−0.7	3.0	7.3
Initial	Lag	0.67	2.06	4.0E+04	0.26	0.01	0.00	0.00	0.00	0.02	−43.3	−5.8	3.3	7.4
		0.73	2.04	nd	0.24	−.01	0.00	0.00	0.00	nd	−43.5	−5.5	3.6	7.3
		22.57	2.12	<1.0E+03	0.28	0.02	0.03	0.03	0.00	0.08	−40.4	−5.4	3.5	7.1
		22.60	2.12	nd	0.27	0.02	0.03	0.03	−0.01	0.07	−35.8	−5.8	3.0	7.7
		46.50	2.08	<1.0E+03	0.28	0.03	0.04	0.05	−0.01	0.10	−37.9	−5.5	3.3	8.3
		46.55	2.06	nd	0.28	0.03	0.04	0.05	−0.01	0.09	−35.8	−5.2	nd	7.5
		70.85	2.06	<1.0E+03	0.31	0.05	0.06	0.06	0.00	0.17	−39.2	−4.9	3.1	7.5
		71.03	2.04	nd	0.34	0.09	0.05	0.05	0.00	0.27	−39.4	−4.7	2.9	7.3
	Exponential	94.2	2.09	5.0E+03	0.32	0.07	0.07	0.07	0.00	0.22	−38.8	−4.6	2.5	7.4
		94.95	2.08	nd	0.32	0.07	0.06	0.06	0.00	0.22	−37.3	−4.2	2.8	6.9
		142.88	2.09	3.0E+04	0.32	0.07	0.08	0.08	0.00	0.22	−36.8	−3.7	3.0	7.2
		142.95	2.06	nd	0.31	0.06	0.07	0.06	0.00	0.19	−36.7	−3.6	2.8	7.8
		190.33	2.10	1.0E+04	0.33	0.08	0.08	0.08	0.00	0.24	−38.9	−3.8	2.9	6.9
		190.38	2.07	nd	0.33	0.08	0.08	0.08	0.00	0.25	−32.6	−3.2	2.8	7.7
		237.40	2.10	7.5E+04	0.33	0.07	0.08	0.08	0.00	0.23	−31.8	−3.3	2.8	8.6
		237.45	2.09	nd	0.32	0.06	0.08	0.08	0.01	0.20	−34.8	−3.2	2.9	7.5
		309.40	2.08	2.6E+05	0.34	0.09	0.09	0.09	0.00	0.25	−29.1	−2.1	nd	7.8
		309.45	2.07	nd	0.34	0.09	0.09	0.08	0.00	0.26	−27.4	−1.7	2.7	7.5
		381.38	2.07	3.5E+04	0.34	0.09	0.09	0.08	0.00	0.26	−34.1	−3.4	2.3	7.2
		381.43	2.06	nd	0.39	0.14	0.09	0.09	0.00	0.35	−27.4	−1.5	2.5	7.0
Main		478.17	1.99	1.6E+07	0.44	0.19	0.15	0.01	0.14	0.43	−27.6	0.3	1.4	6.3
		478.20	1.99	nd	0.43	0.18	0.14	0.01	0.13	0.42	−26.2	0.2	1.2	6.1
		574.00	1.99	2.9E+07	0.48	0.23	0.17	0.01	0.16	0.47	−16.1	4.6	1.0	6.3
		573.92	1.91	nd	0.68	0.43	0.27	0.02	0.25	0.63	−24.9	0.6	−0.7	4.9
		669.82	1.83	nd	1.05	0.80	0.47	0.03	0.44	0.76	−27.9	0.2	−1.8	2.7
		669.88	1.83	nd	1.09	0.83	0.49	0.03	0.46	0.77	−24.4	1.0	−1.7	3.7

nd: not determined.
$\delta^{34}S$ pyrite = −3.7 ± 0.3‰.
[a] U: uninoculated (control) experiments.
[b] SO_4 (total) includes initial SO_4.
[c] SO_4(pyrite) = produced SO_4.
[d] $X = SO_4(\text{pyrite})/SO_4(\text{total})$.

extremely slow (Lloyd, 1968; Zak et al., 1980). Even at pH 2, oxygen isotope exchange is slow (half time > 10 yr, extrapolated from Lloyd, 1968; half time > 10000 yr, extrapolated from Chiba and Sakai, 1985). Thus, sulfate is likely to preserve its oxygen isotope composition once it is formed. Therefore, sulfate derived from leaching of pyrite preserves information about 1) the source of oxygen (in most cases oxygen is either derived from water or from dissolved oxygen), 2) the oxygen isotope fractionation related to biochemical reactions that oxidize pyrite sulfur and sulfur intermediates, and 3) the oxygen isotope exchange processes between intermediate sulfur species (i.e. SO_3^{2-}) and water. So far, most studies have focused on the first two mechanisms, assuming that oxygen isotope exchange between intermediate sulfur compounds and water is of minor importance (Toran and Harris, 1989). Taylor et al. (1984) estimate an isotope fractionation of −11.4‰ for the *Af*-mediated oxidation of pyrite with dissolved oxygen under submersed conditions and an isotope fractionation of +8.9‰ to +10.9‰ for the incorporation of oxygen derived from water under the same conditions. For the same process, Balci et al. (2007) measured fractionations of −9.8‰ to −10.9‰ and +3.5‰, respectively; and Pisapia et al. (2007) measured fractionations of −25‰ and +16‰, respectively. The oxygen and sulfur isotope effects related to the degassing of SO_2 from the solution of the remaining sulfite pool has yet not been investigated, however, due to the kinetic nature of such an escape, one would expect that the sulfur dioxide remaining in solution would be enriched in ^{34}S and ^{18}O (Biegeleisen, 1949).

1.5. Summary

- Nonstoichiometric leaching of pyrite has been observed both in abiotic and biological experiments with *Af*.
- The solution chemistry in the initial and main stage leaching of pyrite by *Af* indicates that there are different biochemical mechanisms between the different leaching modes.
- Sulfur seems to be missing or is present in a yet undetected form.
- Because it is likely that sulfite is one of the sulfur intermediates formed both in abiotic and biological experiments, degassing of sulfur dioxide may account for the missing sulfur, however, this has not been observed so far.
- The sulfur and oxygen isotope composition of formed sulfate could give crucial information for understanding the processes involved, i.e. about the existence of a “missing sulfur pool”.

In this paper, we report the results of experimental work that investigates the potential degassing of sulfur dioxide during pyrite oxidation and its effect on the sulfur and oxygen isotope data of the remaining sulfur species, and we report and interpret sulfur and oxygen isotope analysis of sulfate that was produced in the course of the experiments by Yu et al. (2001).

2. Methods

Stable isotopic compositions of water and dissolved sulfate were measured for the samples collected by Yu et al. (2001), who performed a batch experiment of pyrite oxidation with *Af*. The details of the experimental procedures and the chemical compositional information on the collected samples are described in Yu et al. (2001). The analyzed isotopic compositions include the oxygen isotope composition of water, the oxygen and sulfur isotope composition of sulfate and the sulfur isotope composition of pyrite. The isotopic composition is reported with respect to the standards, Vienna Standard Mean Oceanic

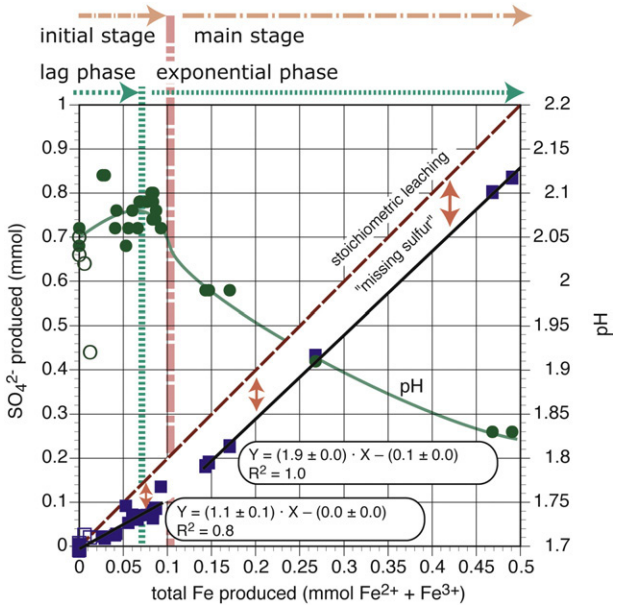

Fig. 2. Relationship between pH, produced SO_4^{2-}, and produced Fe_{tot} during the initial and main stage of pyrite leaching. The dashed vertical lines mark the transition from lag phase to exponential phase of growth and initial stage to main stage of pyrite leaching. The dashed diagonal line depicts a 2:1 ratio for SO_4^{2-}/Fe_{tot} that would be typical for stoichiometric leaching of pyrite. The difference (arrows) between the dashed diagonal line and the linear regression lines corresponds to the amount of "missing sulfur". Note that at the beginning of the main stage of pyrite leaching, no "missing sulfur" is converted to sulfate. During the initial stage of pyrite leaching the pH is higher than the initial pH, but no clear trend can be observed. During the main stage of pyrite leaching, the pH drops continuously. Regression lines are calculated for 95% confidence level. Symbols: crosses: number of cells; filled squares: produced sulfate (*Af*); hollow squares: produced sulfate (uninoculated); filled circles: pH (*Af*); hollow circles: pH (uninoculated).

Water (VSMOW) for oxygen and Vienna Canyon Diablo Troilite (VCDT) for sulfur. The oxygen isotope composition of water was measured using CO_2 equilibration method (Epstein and Mayeda, 1953). Measurements were performed with a stable isotope ratio mass spectrometer (SIR-MS) model VG SIRA 10 at the Postgraduate Research Institute for Sedimentology (PRIS), Reading University, United Kingdom. The reference material used for the calibration of the analytical data was PRIS laboratory standard DW-1 #35 ($\delta^{18}O = -6.7‰$) for oxygen. Dissolved sulfate in the experimental solutions was extracted by precipitation in the form of $BaSO_4$ (Kolthoff et al.; 1969). For sulfur isotope analysis 0.6 mg of the precipitated $BaSO_4$ and 1.2 mg V_2O_5 was mixed in a tin capsule and combusted at 1060 °C in an elemental analyzer (Elemental Combustion System, Costech) to produce SO_2. For oxygen isotope analysis, approximately 0.11 mg of the precipitated $BaSO_4$ and approximately 0.4 mg Ag_2S were transferred to a silver capsule and thermochemically reduced at 1450 °C in the presence of graphite and glassy carbon in the Finnigan Thermal Conversion/Elemental Analyzer (TC/EA) to produce CO. The evolved SO_2 and CO were carried by a helium stream through a GC column, Finnigan Conflo III, and into a Finnigan MAT 253 stable isotope ratio mass spectrometer to measure $\delta^{34}S$ and $\delta^{18}O$, respectively. The sulfur isotope measurements were calibrated with the reference materials RM 8557 (NBS 127; $\delta^{34}S = 20.32‰$), RM 8553 (Soufre de Lacq; $\delta^{34}S = 16.0‰$) and RM 8556 (NBS 123; $\delta^{34}S = -0.3‰$) of National Institute of Standards and Technology. The oxygen isotope measurements were calibrated with NBS 127 ($\delta^{18}O = 8.6‰$ Boschetti and Iacumin, 2005) and JPL laboratory $BaSO_4$ standard ($\delta^{18}O = 11.6‰$). For the measurement of the sulfur isotope composition of pyrite, 0.07 mg of the starting pyrite was mixed with 1.2 mg V_2O_5 and analyzed by following the procedures for sulfur isotope analysis of $BaSO_4$. The standard errors ($\sigma 1$) of the measurements were less than 0.1‰ for $\delta^{18}O_{H_2O}$, 0.2‰ for $\delta^{34}S_{BaSO_4}$, and 0.3‰ for $\delta^{18}O_{BaSO_4}$. The sulfur isotope composition of pyrite was found to be $-3.7 \pm 0.3‰$ ($p = 0.05$, $n = 6$).

Initial experiments were carried out to test the possibility of degassing of SO_2 in abiotic acid pyrite leaching (Table 2a, b, c One set of experiments investigated if abiotic leaching of pyrite with hydrochloric acid produces SO_2 in the headspace of serum bottles flushed with argon gas (Table 2a), a second set tested the same for leaching of pyrite with sulfuric acid (Table 2b). Gas from the headspace from the experiments with hydrochloric acid was flushed by an Ar gas stream into a $Ba(OH)_2$ solution, where SO_2 precipitates as barium sulfite. The formed precipitates were checked by XRD to examine for the possible presence of $BaSO_3$. The presence of SO_2 in the experiments with sulfuric acid was tested by an alternate method: A 10 µl gas sample was drawn from the headspace of the serum bottles with a gas-tight syringe and transferred to a 1 L tedlar sample bag containing pure (99.9995%) helium. The sample bag was connected to a carboxen trap, with gas being drawn from the bag for 2 min to adsorb SO_2 onto the carboxen in the process. Following the sampling process, the trap was isolated and purged with helium prior to performing temperature programmed desorbtion of the carboxen. The desorbed SO_2 was then injected into a prototype gas chromatograph mass spectrometer designed at JPL, Caltech (Shortt et al.; 2005). The detection limit of this mass spectrometer for sulfur dioxide gas is below 10 ppt. The abiotic leaching experiments were performed to investigate if degassing of SO_2 is possible, but do not allow to make conclusive estimates of the quantity of degassed SO_2. In order to do so, a series of experiments that would focus on how experimental parameters affects the degassing would need to be performed. Parameters, such as duration of experiment, flushing of headspace of serum bottles with Ar gas, amount of pyrite and periodic shaking of bottles were chosen arbitrarily. Argon was used to flush the headspace of the serum bottles because we assumed that produced SO_2 would be less prone to be oxidized to sulfate under inert conditions. However, low pO_2 in the headspace may also have reduced the amount of pyrite that was oxidized by the attack of dissolved oxygen, thus could also have led to a lower accumulation of SO_2.

Since only very small amounts of SO_2 were produced in the acid leaching experiments (Table 2b) no isotope analysis could be carried out on the produced gas. Therefore, a third experiment investigated the sulfur isotope effect related to the degassing of SO_2 from sulfurous acid (Table 2c). Twenty-five ml of 0.1 M H_2SO_4–K_2SO_4 solution (pH 1.5) was injected through a septum into an Ar-flushed serum bottle (125 ml) that contained 0.1 g Na_2SO_3. After 5 min, headspace samples were transferred with a gas-tight syringe into the He-flow of the elemental analyzer used for sulfur isotope analysis. The sulfur isotope

Table 2a
Acid pyrite oxidation in sealed serum bottles (125 ml) with HCl

Pyrite powder RM 8455 NIST (g)	HCl–KCl 0.1 M (ml)	pH	Ar[a] (s)	Duration (weeks)	Shaking	Treatment	XRD analysis
0.017	30	1.9	30	3	12 times	Transfer of headspace into $Ba(OH)_2$ trap by Ar stream	$BaCO_3 > 90\%$, no $BaSO_3$
0.05	30	1.9	30	3	12 times		$BaCO_3 > 90\%$, no $BaSO_3$
0.105	30	1.9	30	3	12 times		$BaCO_3 > 90\% + BaSO_3 < 5\%$

[a] The headspace was flushed with Argon gas. This treatment does not ensure that dissolved oxygen is removed from the acid solution.

Table 2b
Acid pyrite oxidation in sealed serum bottles (125 ml) with H_2SO_4

Pyrite powder RM 8455 NIST	H_2SO_4–K_2SO_4 0.1 M (ml)	pH	Ar[a] (s)	Duration (weeks)	Shaking	Treatment	Ion Trap analysis
0 g (blank)	30	1.57	30	3	12 times	Injection of 10 μl headspace gas into 1 L tedlar	No
0 g (blank)	30	1.57	30	3	12 times	sample bag for subsequent analysis by ION Trap	No
0.17 g	30	1.57	30	3	12 times		No
0.05 g	30	1.57	30	3	12 times		No
0.105 g	30	1.57	30	3	12 times		Yes, <10 ppt

[a] The headspace was flushed with Argon gas. This treatment does not ensure that dissolved oxygen is removed from the acid solution.

composition of evolved SO_2 was directly compared to the SO_2 produced by the combustion of Na_2SO_3 (0.3 mg).

3. Results

The results of the isotope measurements are summarized in Table 1. The sulfur isotope composition of samples drops from 3.5‰ at the beginning of the initial stage to 2.4‰ at the end of the initial stage of pyrite leaching (380 h). It further drops from 1.3‰ at the beginning of the main stage of pyrite leaching to −1.7‰ at the end of the experiment (770 h). The sulfur isotope composition of the sulfate from the uninoculated experiments is invariant over the course of the experiment.

The average oxygen isotope composition of sulfate in the initial stage is 7.5‰, ranging from 6.9‰ to 8.6‰. The data scatter and there is no trend. During the main stage of pyrite leaching, the oxygen isotope value of accumulated sulfate drops from 6.2‰ to 3.2‰ at the end of the experiment. The oxygen isotope composition of water rises from −5.6‰ at the beginning to −2.4‰ at the end of the initial stage, as a result of the evaporation of the media also measured by the increase in Mg. During the main stage of pyrite leaching, the oxygen isotope composition of water is between 0.3‰ and 0.6‰, with one outlying data point at +4.6‰.

The initial experiments to explore the possibility of degassing of SO_2 from acid solutions containing pyrite yielded the following results: The flushing of the headspace from the pyrite leaching experiments into a $Ba(OH)_2$ solution caused the formation of precipitates in all 3 experiments. The precipitates were identified by XRD to be dominantly $BaCO_3$ (>90%), most likely derived from CO_2 by contamination with air during the transfer of the headspace into the barium hydroxide trap. $BaSO_3$ (<5%) was identified by XRD in the experiment with most pyrite (0.11 g), whereas no sulfite was detected in the other two experiments (Table 2a). The analysis of the gas in the headspace, with the prototype mass spectrometer, clearly showed a presence of SO_2 (Fig. 3) for the sample containing the most pyrite (0.105 g). In the case of the blanks and the samples with less pyrite (0.017 g, 0.05 g), no SO_2 was detected (Table 2b). The SO_2 level in the experiments with 0.105 g pyrite was very close to the detection limit of the mass spectrometer, thus below 10 ppt. Taking the dilution factor from the sampling procedure into account (10 μl headspace gas injected into a 1 L tedlar sample bag containing pure helium) the concentration of SO_2 in the headspace of the serum bottle is calculated to be below 1 ppm. Repeated analysis of the sample gas from the tedlar bag showed a decrease in the amount of detected SO_2 (Fig. 3). This implies that SO_2 is lost over time, most likely due to adsorption on the sample bag. Thus, we may underestimate the actual amount of SO_2 in the serum bottles. The sulfur dioxide that evolved from the experiment, where sodium sulfite was dissolved in acid, was depleted in ^{34}S by −12±2‰ with respect to the Na_2SO_3 used (Table 2c).

4. Discussion

The collected sulfate samples consist of initial sulfate in the experiment and sulfate accumulated in solution during the progressive leaching of pyrite. Thus, the sulfur and oxygen isotope composition measured does not reflect the isotope composition of sulfate produced at a certain time, but an average of the isotope composition of initial sulfate and the isotope composition of sulfate produced between the start of the experiment and the time the sample was taken. In order to derive the isotope composition of produced sulfate from our data, we plot the isotope data against the relative amount of produced sulfate to total sulfate (Fig. 4 and 6) according to:

$$X = \text{produced sulfate}/(\text{initial sulfate} + \text{produced sulfate}).$$

At the start of the experiment, where all sulfate is initial sulfate, X equals 0, towards the end of the experiment, where the amount of produced sulfate is much larger than the initial amount of sulfate, X approaches 1. In such plots, linear trends in the isotope composition of sulfate indicate the production of sulfate with a constant isotope composition, and this composition can be deduced by extrapolation of the regression line to $X=1$.

Fig. 4 shows linear isotope trends with respect to the relative amount of produced sulfate. During the main stage of pyrite leaching, there is a strong linear correlation between the sulfur isotope composition of sulfate in solution and X ($R^2=0.99$). Extrapolation of the regression line for the main stage to $X=1$ indicates the production of sulfate with a $\delta^{34}S$ of −3.9±1.8‰ for the main stage which is close to the $\delta^{34}S$ of pyrite of −3.7±0.3‰. No sulfur isotope fractionation between pyrite and produced sulfate in aerobic leaching by *Af* was observed in the experiments by Balci et al. (2007) for the main stage of pyrite leaching as well.

During the initial stage of pyrite leaching, the sulfur isotope trend is not as steep as during the main stage of pyrite leaching, and there is only a weak linear correlation between the sulfur isotope data and X ($R^2=0.60$), indicating that processes other than the addition of sulfur from pyrite leaching contribute to the sulfur isotope composition of produced sulfate, i.e. that sulfur isotope fractionation occurs. This is confirmed by extrapolating the regression line for the main stage of pyrite leaching to $X=0$: If the sulfur isotope composition of produced sulfate would have been the same over the whole course of the experiment, the initial composition would be 5.1±1.0, which is significantly different from the actual measured initial composition of 3.5±0.3‰. Thus, sulfate produced during the initial stage of pyrite

Table 2c
Sulfur isotope effect by degassing of SO_2 from a Na_2SO_3 solution by acidification with H_2SO_4 in a sealed serum bottle (125 ml)

Na_2SO_3	Ar[a]	H_2SO_4–K_2SO_4 0.1 M	pH	Duration	Treatment	Analysis	$\delta^{34}S$ (SO_2)–$\delta^{34}S$ (Na_2SO_3)[b]
0.1 g	30 s	25 ml	1.5	5 min	Injection of headspace into Elemental Analyzer	IRMS	−12±2‰

[a] The serum bottle was flushed with Argon gas after addition of Na_2SO_4. The bottle was capped and the H_2SO_4 solution injected with a syringe.
[b] Direct comparison of 10 replicates (1σ) to SO_2 produced by combustion of 0.3 mg Na_2SO_3.

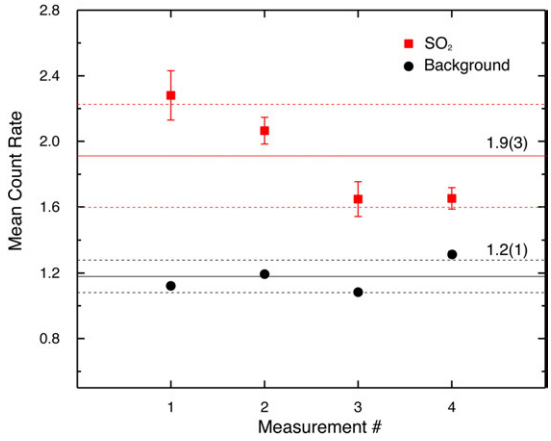

Fig. 3. Mean value of the count rate for four chromatography measurements from the experiment with 0.105 g pyrite. In squares, mean value of the SO_2 count rate for; in circles mean value of the background count rate. The sulfur dioxide signal is averaged over 30 time units and the background signal over 180 time units. The error bars for SO_2 correspond to the standard deviation (1σ) of one measurement. The solid and two broken lines show mean value and standard deviation (1σ) among the four measurements. The standard deviation of the background measurements is smaller than the size of the circles. The measurements were carried out successively form the same sample bag; duration between measurements was half an hour. We believe that the drop of the concentration of SO_2 from the first (1) to the last analysis (4) is due to absorption/reaction of SO_2 with the walls of the sample bag.

leaching is enriched in ^{34}S compared to pyrite. Pisapia et al. (2007) found only a minor enrichment in ^{34}S ($\Delta^{34}S_{sulfate-pyrite}$=+0.4‰) for sulfate produced by nonstoichiometrical leaching of pyrite by *Af*. However, the nonstoichiometrical leaching process investigated by Pisapia et al. (2007) is strongly different from the one by Yu et al. (2001); Pisapia et al. (2007) find excess sulfate formed in the initial stage of pyrite leaching. Together with the increase in sulfate, they observe an increase in Cu^{2+}. This could indicate a preferential leaching of copper–iron sulfide impurities from pyrite. Such a leaching process would be entirely different from actual pyrite leaching; for instance chalcopyrite ($CuFeS_2$) is leached by the polysulfide-mechanism (Schippers and Sand, 1999). It is likely, that in such a case, different nonstoichiometrical patterns and isotope effects would be observed.

Fig. 5 shows the oxygen isotope trends for sulfate and for water. The nonlinear trend in the oxygen isotope composition of water is due to the fact that sulfate accumulation is not linear with time. Thus, small sulfate accumulation towards the end of the initial stage of pyrite leaching causes the oxygen isotope curve for water to appear steeper, while high sulfate production during the main stage of pyrite causes the oxygen isotope curve for water to appear more flat.

During the main stage of pyrite leaching, the oxygen isotope composition of sulfate shows a clear trend and correlates well with X (R^2=0.91). By extrapolation of the regression line to X=1 a $\delta^{18}O$ of 1.3±2.6‰ for produced sulfate results, which is close to the oxygen isotope composition of water for the latter part of the experiment (0‰ to 1‰). Dependent on the pyrite oxidation pathway, different oxygen isotope fractionations can be determined, the range for the isotope fractionation related to the incorporation of oxygen derived from H_2O is from +4.1 to −6‰ (Taylor et al., 1984) and references therein. For the main stage of pyrite leaching by *Af*, Balci et al. (2007) found an enrichment in ^{18}O of +3.5‰ in sulfate compared to water. The discrepancy between the results of Balci et al. (2007) and ours may be partly due to the use of different values for the standard NBS 127: Balci et al. (2007) use the internationally accepted value of +9.3‰ while we use a value of +8.6‰ which has been suggested by Boschetti and Iacumin (2005). We prefer the latter value for NBS 127 since it has been determined by direct comparison to water standards (Böhlke et al.; 2003). This is important because most oxygen in sulfate from pyrite oxidation is derived from water. Using the value +9.3‰ for NBS 127, the oxygen isotope fractionation in the main stage of our experiment would be calculated as 2.0±2.6‰, which, compared to the result of Balci et al. (2007) is within error.

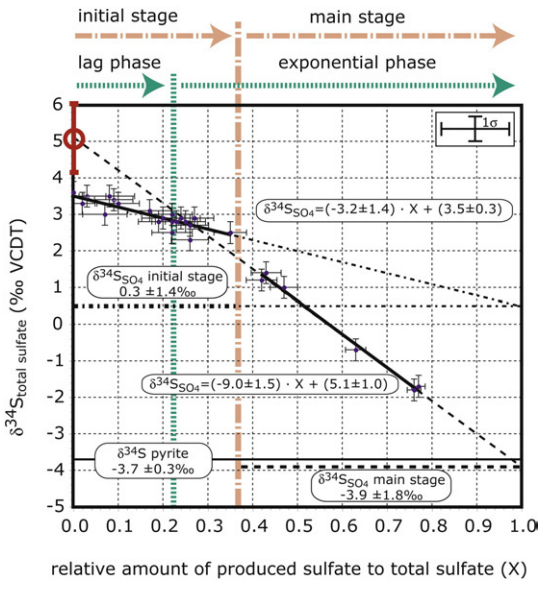

Fig. 4. Relationship between sulfur isotope composition of sulfate to the relative amount of produced sulfate to total sulfate. The sulfur isotope trends for the initial stage of pyrite leaching are different from the trend for the main stage. The dashed lines show the sulfur isotope composition of sulfate that is produced in the initial stage and the main stage. The dashed vertical lines mark the transition from lag phase to exponential phase of growth and initial stage to main stage of pyrite leaching. Regression lines are calculated for 95% confidence level. Symbols: filled circles: $\delta^{34}S$ of total sulfate (*Af*); hollow circles: $\delta^{34}S$ of total sulfate (uninoculated). The large symbol at X=0 and $\delta^{34}S$=5.1 depicts the intercept for the regression line for the exponential phase.

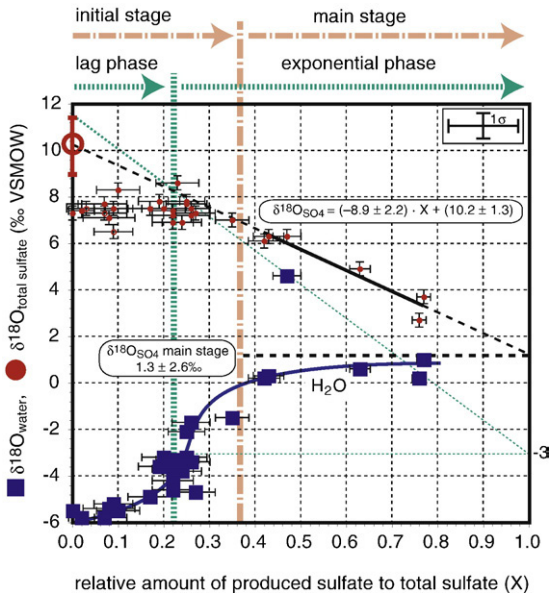

Fig. 5. Relationship between oxygen isotope composition of sulfate and water to the relative amount of produced sulfate to total sulfate. The oxygen isotope trends for the initial stage of pyrite leaching are different from the trend for the main stage. The dashed line shows the oxygen isotope composition of sulfate that is produced in the main stage. The dashed vertical lines mark the transition from lag phase to exponential phase of growth and initial stage to main stage of pyrite leaching. Regression lines are calculated for 95% confidence level. Symbols: filled circles: $\delta^{18}O$ of produced sulfate (*Af*); hollow circles: $\delta^{18}O$ of produced sulfate (uninoculated); filled squares: $\delta^{18}O$ of water (*Af*) The large symbol at X=0 and $\delta^{18}O$=5.1 depicts the intercept for the regression line for the exponential phase (see text).

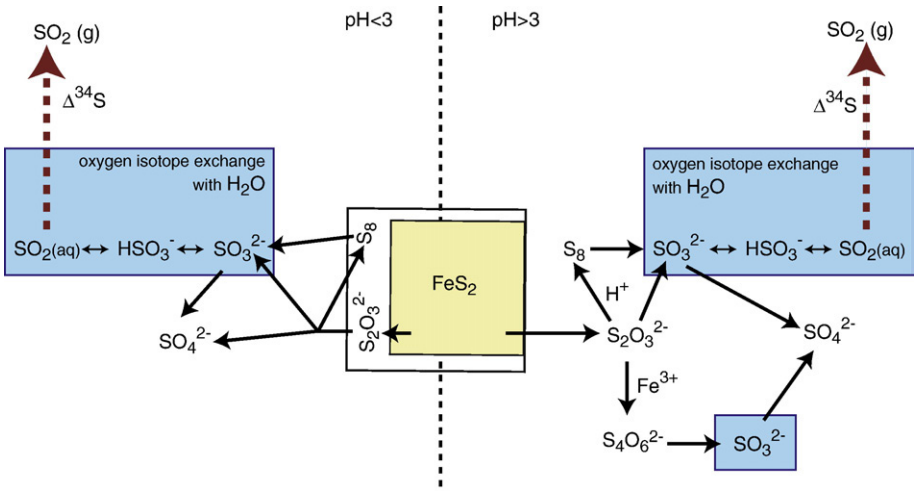

Fig. 6. Thiosulfate pathway (modified from Druschel and Borda, 2006): Formation of a Fe-SSO_3 surface structure, which can detach as thiosulfate (right side, occurs at pH>3 Luther, 1987; Williamson and Rimstidt, 1993) or as sulfite/sulfate under the production of a residual sulfur pool (left side, likely to occur at pH below 3). Left side: Formation of sulfate or sulfite under the production of monosulfide, which may be oxidized to elemental sulfur or sulfoxyanion species (Druschel and Borda, 2006). Right side: Release of thiosulfate ($S_2O_3^{2-}$) with subsequent competition between two reactions: Decomposition into elemental sulfur and sulfite (SO_3^{2-}) under acidic conditions or formation of tetrathionate ($S_4O_6^{2-}$) in the presence of ferric iron (Fe^{3+}). However, unless the supply of ferric iron is limited, the latter reaction dominates (Williamson and Rimstidt, 1993). Dark boxes: Sulfite is an important intermediate in most of the depicted pathways. Under acidic conditions, it rapidly equilibrates oxygen isotopes with water and allows for degassing of sulfur dioxide (SO_2), which is driven by the pH and venting conditions. Loss of SO_2 (dashed arrows, $\Delta^{34}S$) or accumulation of elemental sulfur (S_8) could lead to a difference between the sulfur isotope composition of sulfate in solution and leached pyrite.

The oxygen isotope data for sulfate from the initial stage of pyrite leaching scatter strongly, there is no linear correlation between the oxygen isotope composition of sulfate and X (R^2=0.04) despite a progressive 6‰ increase of water $\delta^{18}O$. This indicates that there may be a difference in the processes that control the oxygen isotope composition of produced sulfate for the initial stage of pyrite leaching compared to the mechanism in the main stage, where the oxygen isotope composition of produced sulfate is similar to the oxygen isotope composition of water. We explore this by extrapolating the regression line for the main stage of pyrite leaching to X=0: If the oxygen isotope composition of produced sulfate would be derived from water with an isotope composition of 1.3‰, the oxygen isotope composition of the initial sulfate would be 10.18±1.3, which is significantly different from the actual measured initial composition of 7.4± 0.3‰. Taking into account that the oxygen isotope composition of water during the initial stage was depleted in ^{18}O compared to the water of the main stage, the back calculated initial value would be even higher. For example, using an isotope composition of −3‰ for sulfate produced during the phase X=0 to X=0.22, followed by sulfate with a composition of 1.3‰, an oxygen isotope of initial sulfate of more than 11‰ would result (Fig. 6). This is clear evidence that, sulfate produced during the initial stage of pyrite leaching is enriched in ^{18}O compared to water. Since there is no clear trend in the oxygen isotope composition of sulfate produced in the initial stage its average oxygen isotope composition must be roughly equal to the isotope composition of initial sulfate (7.4±0.3‰), however, the scatter in the data shows that the actual oxygen isotope composition of produced sulfate varies strongly.

The sulfur isotope composition of produced sulfate from the initial stage can be estimated by extrapolation of the regression lines for the data to X=1. However, this estimate must be taken with caution, since there is scatter in the data the linear correlation between X and sulfur isotopes is weak (R^2=0.60). Extrapolation of the regression lines to X=1 indicates the production of sulfate with a $\delta^{34}S$ of 0.3±1.4‰ for the initial stage. This indicates the formation of two sulfur pools, sulfate enriched in ^{34}S by roughly 4.0‰ compared to pyrite and another "missing sulfur" pool, which is depleted in ^{34}S with respect to pyrite. Using the nonstoichiometric relationship between sulfate and total iron of 1.1 the isotope composition of the "missing sulfur" pool can be estimated to be around −9.0‰. Thus, the "missing sulfur" is depleted in ^{34}S by roughly −5.3‰ relative to pyrite and by −9.3‰ relative to sulfate.

5. Interpretation

5.1. Leaching mode of pyrite in the initial stage and degassing of SO_2

Our data show that the initial stage of pyrite leaching by *Af* produces sulfate that is different in its oxygen and sulfur isotope composition from the one produced in the main stage of pyrite leaching. This is evidence for differences in the mechanism of the leaching process (i.e. kinetics and/or reaction pathways) that need to be explained in the context of the observation of the changes in the solution chemistry (Fe species, pH and sulfate–iron ratio), microbial growth and abiotic pyrite oxidation mechanism.

Actual degassing of sulfur dioxide related to abiotic or biological leaching of pyrite has not been recorded so far. A correlation between the population size of *Af* in acid sulfate soils and the evolution of SO_2 has been observed by Dürr et al. (2004). Emission of sulfur dioxide from sulfuric soils is related to the oxidation of pyrite; the mechanism causing these emissions is currently not resolved (Macdonald et al., 2004; Kinsela et al., 2007). Descostes et al. (2004) report SO_4^{2-}/Fe_{tot} ratios of 1.5 to 1.6 at pH of 1.2 to 2 in abiotic experiments with perchloric and hydrochloric acid and present a data compilation that indicates that the observed ratio depends on the pH of the solution. Since the degassing rate of SO_2 is higher at lower pH, Descostes et al. (2004) suggest that the "missing sulfate" may have degassed as sulfur dioxide (SO_2). Our initial experiments with acid leaching of pyrite by hydrochloric and sulfuric acid show that small quantities of SO_2 can be produced. This provides evidence for the formation of sulfite species during abiotic leaching of pyrite but no proof that degassing of SO_2 accounts for the nonstoichiometric sulfate:iron ratios in acid pyrite leaching experiments. Druschel and Borda (2006) showed that nonstoichiometric sulfate:iron ratios can be caused by other processes: At pH below 3, Fe-SSO_3 surface structures on the pyrite surface are the first product of pyrite leaching (Fig. 6), allowing subsequent reactions to break the S–S bond (Rimstidt and Vaughan, 2003), releasing sulfate or sulfite species to the solution (Borda et al.,

2003). The abiotic oxidation of pyrite to sulfite is composed by two half-reactions (Rimstidt and Vaughan, 2003):

$$\text{Cathode site of pyrite}: 3/2O_2 + 6H^+ \Rightarrow 3H_2O \quad (1.1)$$

$$\text{Anode site of pyrite}: FeS_2 + 3H_2O \Rightarrow Fe^{2+} + S^0 + SO_3^{2-} + 6H^+. \quad (1.2)$$

And, reactions to sulfate, respectively are:

$$\text{Cathode site of pyrite}: 2O_2 + 8H^+ \Rightarrow 4H_2O \quad (2.1)$$

$$\text{Anode site of pyrite}: FeS_2 + 4H_2O \Rightarrow Fe^{2+} + S^0 + SO_4^{2-} + 8H^+. \quad (2.2)$$

Either sulfite or sulfate could be the reaction product and both reactions are pH neutral. This scenario includes the formation of monosulfide, which may be oxidized to elemental sulfur and sulfur oxyanion species (Druschel and Borda, 2006). If not all monosulfide is subsequently oxidized to sulfate, this chemical pathway can cause nonstoichiometric SO_4^{2-}:Fe_{tot} ratios as low as 1. However, detectable amounts of those sulfur species should remain in the solution or on the pyrite surface. Descostes et al. (2004) did not detect any dissolved sulfur species besides sulfate by ion chromatography; the presence of elemental sulfur was not investigated in their experiments. In the here investigated pyrite leaching experiments with *Af* by Yu et al. (2001) neither elemental sulfur nor dissolved sulfur species besides sulfate were detectable, and the "missing sulfur" was not converted to sulfate at the beginning of the main stage of pyrite leaching (Fig. 2), but remained missing. This leads us to the conclusion that accumulation of sulfite in the solution with subsequent degassing of SO_2 is the best hypothesis to explain the observations from the initial stage of pyrite leaching by *Af*. There are two major differences between abiotic and biological nonstoichiometric leaching of pyrite: For biological leaching at pH 2 both leaching rate (observed from the uninoculated experiments) and size of "missing sulfur pool" (SO_4^{2-}/Fe_{tot} ratio of 1.1 in the presence of *Af* and 1.6 for abiotic leaching Descostes et al., 2004) are larger. We believe that this is due to microbial oxidation of elemental sulfur to sulfite as main energy source for *Af* Eq. (3.3) that follows the abiotic attack of the pyrite surface Eqs. (3.1) and (3.2).

$$FeS_2 + 3/2O_2 \Rightarrow Fe^{2+} + S^0 + SO_3^{2-} \quad (3.1)$$

$$FeS_2 + 2O_2 \Rightarrow Fe^{2+} + S^0 + SO_4^{2-} \quad (3.2)$$

$$S^0 + O_2 + H_2O \Rightarrow H^+ + HSO_3^- (\Delta G^\circ = -272.2 kJ/mol O_2). \quad (3.3)$$

This removes sulfur coatings from reactive pyrite sites, thus allowing for faster leaching of pyrite and promotes formation of sulfite species. If sulfite oxidation Eq. (3.4) is not accelerated accordingly, more SO_2 will degas Eq. (3.5).

$$SO_3^- + 1/2O_2 \Rightarrow SO_4^{2-} (\Delta G^\circ = -258 kJ/mol SO_3^-; -516 kJ/mol O_2) \quad (3.4)$$

$$H^+ + HSO_3^- \Rightarrow SO_2 + H_2O. \quad (3.5)$$

Eqs. (3.1) and (3.2) describe the abiotic leaching of pyrite at pH<3, Eq. (3.3) the oxidation of elemental sulfur by dissolved oxygen, which is accelerated in the presence of *Af*, Eq. (3.4) the oxidation of sulfite to sulfate, and Eq. (3.5) the formation and degassing of sulfur dioxide from sulfite under acidic conditions. This sequence of reactions leads to the following theoretical net reaction:

$$FeS_2 + 3O_2 \Rightarrow Fe^{2+} + SO_4^{2-} + SO_2(g). \quad (3.6)$$

The net reaction Eq. (3.6) is consistent with the observations from the chemistry of the solution: Ferrous iron is the main dissolved iron species, it is not in a stoichiometric relationship to the amount of dissolved sulfate, and the reaction does not alter the pH of the solution. The degassing of sulfur dioxide explains why the "missing" amount of sulfur does not reappear in the main stage of pyrite leaching.

This scenario is supported by the sulfur and oxygen isotope data from the initial stage of pyrite leaching by *Af*. The "missing sulfur" pool is depleted in ^{34}S by roughly −9.3‰ relative to the accumulating sulfate, which corresponds well with the isotope depletion of −12±2‰ for SO_2 evolved from sodium sulfite that was dissolved in acid (Table 2c). Similarly, degassing of SO_2 should cause enrichment of ^{18}O in the remaining sulfite pool. At low pH, oxygen isotope exchange between sulfite species and water is very rapid (Betts and Voss, 1970; Horner and Connick, 2003), however, the exact oxygen isotope fractionation between sulfite and water is currently not known. The equilibrium oxygen isotope fractionation between sulfur dioxide and water vapor is +24.3‰ (Holt et al., 1983). At pH 7 sulfite is enriched in ^{18}O at least by 11‰ with respect to water (Brunner et al., 2006). This implies, that if sulfite species are present, and exist long enough to allow for oxygen isotope exchange, sulfite would be enriched in ^{18}O compared to water. The possibility of oxygen isotope fractionation between sulfite and water has been mentioned by Lloyd (1968) and it has been speculated that this process may be responsible for the oxygen isotope effects observed in sulfate related to dissimilatory sulfate reduction and disproportionation of sulfur (e.g. Fritz et al., 1989; Böttcher et al., 2005; Brunner et al., 2005; Turchyn and Schrag, 2006). Thus, both degassing of SO_2 and oxygen isotope exchange between water and sulfite should lead to sulfite enriched in ^{18}O compared to water. Correspondingly, sulfate derived from the oxidation of this sulfite should be enriched in ^{18}O as well. This accords well with the sulfate produced during the initial stage of pyrite leaching which is enriched in ^{18}O compared to water by roughly +10‰. The strong scatter in the data may be due to the competition between processes deriving oxygen from water and processes that derive oxygen from O_2 for the oxidation of the sulfur species to sulfate.

5.2. Leaching mode of pyrite in the initial stage and degassing of SO_2

During the main stage, pyrite sulfur is almost quantitatively converted to sulfate, according to the net reaction

$$FeS_2 + 15/4O_2 + 1/2H_2O \Rightarrow Fe^{3+} + 2SO_4^{2-} + H^+. \quad (4.1)$$

This reaction is composed of the abiotic attack of ferric iron on pyrite, where the oxygen of sulfate is derived from water

$$FeS_2 + 14Fe^{3+} + 8H_2O \Rightarrow 15Fe^{2+} + 2SO_4^{2-} + 16H^+ \quad (4.2)$$

and by the oxidation of ferrous iron with dissolved oxygen to ferric iron, a reaction which is catalyzed by *Af* (ΔG° = −33 kJ/mol Fe^{2+}; −131.7 kJ/mol O_2)

$$15Fe^{2+} + 15/4O_2 + 15H^+ \Rightarrow 15Fe^{3+} + 15/2H_2O. \quad (4.3)$$

Due to the quantitative conversion of sulfur from pyrite to sulfate, no sulfur isotope fractionation is observed, and the oxygen isotope composition is close to that of water.

5.3. Offset between lag phase of growth of Af and change in leaching stage of pyrite

The cell counts of bacteria in solution indicate that the transition between the lag phase of growth (no increase in cell counts) and the exponential phase of growth (linear increase in counts on a logarithmic scale) occurs at a time around 70 h of incubation (Fig. 1). The major change in the solution chemistry and in the isotope composition of produced sulfate, however, takes place at around 400 h of incubation. This raises the question if the chemical changes are directly related to

changes in the growth phases of the bacteria. During the initial stage of pyrite leaching, the major increase in sulfate and iron in solution occurs in the first 100 h, while in the time between 100 and 400 h, the sulfate and iron concentration remains almost constant (Fig. 1). This indicates that the leaching mode of Af during the lag phase is replaced by a leaching mode that belongs to the initial part of the exponential growth phase. Since ferrous iron is readily available in the solution, the cells in solution are likely to gain their energy from its oxidation to ferric iron Eq. (4.3). In fact, the cell count just before 400 h shows a decrease (Table 1), which we interpret as adaptation to the new metabolic pathway. This reduction is similar to the reduction at the beginning of the experiment when an inoculum taken from an exponential growth culture adapts to pyrite oxidation in the absence of ferrous iron. At the start of the exponential growth, the number of bacteria in solution is very low and the rate of production of ferric iron is smaller than the rate of ferric iron reduction in the abiotic attack on pyrite Eq. (4.2). Therefore, ferrous iron remains the dominant iron species in solution. In the absence of ferric iron that would oxidize sulfite, sulfur dioxide degassing and thus nonstoichiometric leaching of pyrite may still occur, however, the very small amount of change in the concentration of sulfate and ferrous iron during the time between 100 and 400 h makes it hard to explore this in more detail. Thus, there is an offset between the lag phase of growth of *Af* and the change in the solution chemistry of pyrite; however, the chemical changes are linked to the change in the growth phases.

During the lag phase, the bacteria are attached to the pyrite surface, where elemental sulfur is formed, and the oxidation of this elemental sulfur seems to be the energy source. Preferred oxidation of elemental sulfur over ferrous iron, as is the case in the initial stage of pyrite leaching by *Af*, has been observed before at pH values below 1.3 (Sand, 1989). Interestingly, the production rate of ferrous iron and sulfate declines almost to zero after the end of the lag phase in growth of *Af* (70–100 h). This indicates that the nonstoichimetric pyrite leaching mechanism was limited, either by substrate availability (i.e. reactive sites on the pyrite surface) or by accumulated products, i.e. ferrous iron and sulfite, triggering changes in the metabolic activity of *Af*. Inhibition of enzymatic activities of *Af* has been observed for sulfite (Sugio et al., 1994; Takeuchi and Suzuki, 1994; Rohwerder and Sand, 2003), for ferrous iron (Sugio et al., 1990; Sugio et al., 1992; Das et al., 1993) and for pH below 1.3 (Sand, 1989). In the initial stage of pyrite leaching of the Yu et al. (2001) experiments, the sulfite concentrations were below the detection limits (<1 ppm), the concentration of ferrous iron reached 2 mM and the pH stayed above 2. Thus, accumulation of ferrous iron is the most likely candidate that may have caused inhibition of certain metabolic processes of *Af*. Sugio et al. (1990) found that hydrogen sulfide:ferric iron oxidoreductase and sulfite:ferric iron oxidoreductase were completely inhibited by 20 mM and 1 mM Fe^{2+}, respectively. The use of elemental sulfur as energy source by *Af* was completely inhibited above 108 mM of Fe^{2+}. Thus, the accumulation of ferrous iron may have a negative influence on the capability of *Af* to oxidize sulfur compounds. Margalith et al. (1966) observed that the oxidation rate of Fe^{2+} by *Af* decreased in the presence of elemental sulfur, indicating that there might be a competition between microbial oxidation of sulfur compounds and oxidation of ferrous iron. Recent investigations into the protein expression during growth of *Af* on ferrous iron and sulfur compounds (Brasseur et al., 2004; Ramírez et al., 2004; Yarzábal et al., 2004) confirm the strong influence of the concentration of Fe^{2+} on the metabolic activity of *Af*. Thus, high concentrations of ferrous iron may trigger the transition from a sulfur oxidation mechanism to a mechanism where oxidation of ferrous iron dominates. The transition between initial and main stage of pyrite leaching by *Af* sheds light on an interesting physiological aspect: A mode, where bacteria gain energy by oxidation of elemental sulfur ($\Delta G^0 = -272.2$ kJ/mol O_2) but show little growth in population due to a slow abiotic pyrite leaching mechanism is switched into a mode, where bacteria gain a smaller amount of energy by the oxidation of ferrous iron ($\Delta G^0 = -131.7$ kJ/mol O_2), but induce much faster pyrite leaching rates due to the production of ferric iron. Compared to the main stage, where bacteria mainly depend on the availability of ferrous iron from the solution, the initial phase of pyrite oxidation seems to be a much more secure way to establish a sustainable population. Thus, the intriguing change in the leaching mechanism of pyrite by *Af* may reflect a survival and growth strategy.

6. Outlook

This work puts emphasis on four aspects related to oxidation of pyrite by *Af*: The importance of the initial stage of pyrite leaching, the degassing of sulfur dioxide during biological and abiotic acid pyrite leaching, the importance of sulfite as an intermediate in the oxidation of pyrite and the influence of ferrous iron on the metabolic activity of *Af*. None of these aspects is new in the literature, however, yet, they have not been explored thoroughly. We hope that our work stimulates further research in this direction.

7. Conclusions

Sulfur and oxygen isotope analysis of sulfate that is produced during pyrite leaching by *Af* confirms that the leaching mechanism during the initial stage of pyrite leaching is different from the mechanism in the main stage. Enrichment in the ^{18}O of produced sulfates in the initial stage indicates the formation of sulfite as an intermediate that is not immediately converted to sulfate, therefore allowing for oxygen isotope exchange between sulfite species and water and allowing for degassing of sulfur dioxide under acidic conditions. Loss of ^{34}S-depleted SO_2 causes enrichment of ^{34}S in formed sulfate and explains nonstoichiometric sulfur–iron ratios during the initial stage of pyrite leaching. This is consistent with observed degassing of SO_2 in abiotic acid pyrite leaching experiments.

The transition from initial stage of pyrite stage may be triggered by the accumulation of ferrous iron. It defines a fundamental change in the growth strategy of *Af*. A mode, where bacteria gain energy by oxidation of elemental sulfur ($\Delta G^0 = -272.2$ kJ/mol O_2) but show little growth in population due to a slow abiotic pyrite leaching mechanism is switched into a mode, where bacteria gain a smaller amount of energy by the oxidation of ferrous iron ($\Delta G^0 = -131.7$ kJ/mol O_2), but induce much faster pyrite leaching rates due to the production of ferric iron.

Acknowledgements

This research was carried out by the Jet Propulsion Laboratory (JPL), California Institute of Technology, under contract with the National Aeronautics and Space Administration (NASA) with support from JPL's Research and Technology Development Program via a grant to MC. The visiting program of Kangwon National University Research Fund supported J-Y. Yu's visit to PRIS in 1998 and to JPL in 2005. We greatly acknowledge M. Isaacs in PRIS for helping in isotopic analysis of water, B. Abbey for doing the XRD analysis and G. L. Arnold for discussions and help with statistics. We are very grateful for the thorough review by K. W. Mandernack that helped focus and strengthen this manuscript.

References

Balci, N., Shanks, W.C., Mayer, B., Mandernack, K.W., 2007. Oxygen and sulfur isotope systematics of sulfate produced by bacterial and abiotic oxidation of pyrite. Geochimica et Cosmochimica Acta. doi:10.1016/j.gca.2007.04.017.

Betts, R.H., Voss, R.H., 1970. The kinetics of oxygen exchange between the sulfite ion and water. Canadian Journal of Chemistry 48, 2036–2041.

Biegeleisen, J., 1949. The relative velocities of isotopic molecules. Journal of Chemical Physics 17, 675–678.

Böhlke, J.K., Mroczkowski, S.J., Coplen, T.B., 2003. Oxygen isotopes in nitrate: new reference materials for $^{18}O:^{17}O:^{16}O$ measurements and observation on nitrate-water equilibration. Rapid Communications in Mass Spectrometry 17, 1835–1846. doi:10.1002/rcm.1123.

Borda, M.J., Strongin, D.R., Schoonen, M.A., 2003. A vibrational spectroscopic study of the oxidation of pyrite by ferric iron. American Mineralogist 88 (8–9), 1318–1323.

Boschetti, T., Iacumin, P., 2005. Continuous-flow $d^{18}O$ measurements: new approach to standardization, high-temperature thermodynamic and sulfate analysis. Rapid Communications in Mass Spectrometry 19, 3007–3014. doi:10.1002/rcm.2161.

Böttcher, M.E., Thamdrup, B., Gehre, M., Theune, A., 2005. 34S/32S and 18O/16O fractionation during sulfur disproportionation by *Desulfobulbus propionicus*. Geomicrobiology Journal 22, 219–226. doi:10.1080/01490450590947751.

Brasseur, G., Levican, G., Bonnefoy, V., Holmes, D., Jedlicki, E., Lemesle-Meunier, D., 2004. Apparent redundancy of electron transfer pathways via bc1 complexes and terminal oxidases in the extremophilic chemolithoautotrophic *Acidithiobacillus ferrooxidans*. Biochimica et Biophysica Acta 1656, 114–126.

Brunner, B., Bernasconi, S.M., Kleikemper, J., Schroth, M.H., 2005. A model for oxygen and sulfur isotope fractionation in sulfate during bacterial sulfate reduction processes. Geochimica et Cosmochimica Acta 69 (20), 4773–4785. doi:10.1016/j.gca.2005.04.017.

Brunner, B., Mielke, R.E., Coleman, M., 2006. Abiotic oxygen isotope equilibrium fractionation between sulfite and water. Eos Trans. AGU 87 (52) Fall Meet. Suppl., Abstract V11C-0601.

Chiba, H., Sakai, H., 1985. Oxygen isotope exchange rate between dissolved sulfate and water at hydrothermal temperatures. Geochimica et Cosmochimica Acta 49, 993–1000.

Chu, X., Ohmoto, H., Cole, D.R., 2004. Kinetics of sulfur isotope exchange between aqueous sulfide and thiosulfate involving intra- and intermolecular reactions at hydrothermal conditions Chemical Geology 211, 217–235. doi:10.1016/j.chemgeo.2004.06.013.

Das, A., Mishra, A.K., Roy, P., 1993. Inhibition of thiosulfate and tetrathionate oxidation by ferrous iron in *Thiobacillus ferrooxidans*. FEMS Microbiology Letters 112, 67–72.

Descostes, M., Vitorge, P., Beaucaire, C., 2004. Pyrite dissolution in acidic media. Geochimica et Cosmochimica Acta 68 (22), 4559–4569. doi:10.1016/j.gca.2004.04.012.

Druschel, G., Borda, M., 2006. Comment on "Pyrite dissolution in acidic media" by M. Descostes, P. Vitorge, and C. Beaucaire. Geochimica et Cosmochimica Acta 70, 5246–5250. doi:10.1016/j.gca.2005.07.023.

Dürr, M., Kinsela, A., Macdonald, B.C.T., White, I., 2004. Influence of land use on the emission of sulfur dioxide from acid sulfate soils. SuperSoil 2004: 3rd Australian New Zealand Soils Conference, 5–9 December 2004. University of Sydney Australia.

Eccleston, M., Kelly, D.P., 1978. Oxidation kinetics and chemostat growth kinetics of *Thiobacillus ferrooxidans* on tetrathionate and thiosulfate. Journal of Bacteriology 134 (3), 718–727.

Epstein, S., Mayeda, T.K., 1953. Variation of 18O content of waters from natural sources. Geochimica et Cosmochimica Acta 4, 213–224.

Friedrich, C.G., Rother, D., Bardischewsky, F., Quentmeier, A., Fischer, J., 2001. Oxidation of reduced inorganic sulfur compounds by bacteria: emergence of a common mechanism? Applied and Environmental Microbiology 67 (7), 2873–2882. doi:10.1128/AEM.67.7.2873-2882.2001.

Fritz, P., Basharmal, G.M., Drimmie, R.J., Ibsen, J., Qureshi, R.M., 1989. Oxygen isotope exchange between sulphate and water during bacterial reduction of sulphate. Chemical Geology (Isotope Geoscience Section) 79, 99–105.

Hirose, T., Suzuki, H., Inagaki, K., Tanaka, H., Tano, T., Sugio, T., 1991. Inhibition of sulfur use by sulfite ion in *Thiobacillus ferrooxidans*. Agricultural and Biological Chemistry 55 (10), 2479–2484.

Holt, B.D., Cunningham, P.T., Engelkemeir, A.G., Graczyk, D.G., Kumar, R., 1983. Oxygen-18 study of nonaqueous-phase oxidation of sulfur dioxide. Atmospheric Environment 17 (3), 625–632.

Horner, D.A., Connick, R.E., 2003. Kinetics of oxygen exchange between the two isomers of bisulfite ion, disulfite ion (S2O52-), and water as studied by oxygen-17 nuclear magnetic resonance spectroscopy. Inorganic Chemistry 42 (6), 1884–1894. doi:10.1021/ic020692n.

Kinsela, A.S., Reynolds, J.K., Melville, M.D., 2007. Agricultural acid sulfate soils: a potential source of volatile sulfur compounds? Environment & Chemistry 4, 18–25. doi:10.1071/EN06071.

Kolthoff, J.M., Meehan, E.J., Sadell, E.B., Bruckenstein, S., 1969. Quantitative Chemical Analysis, 4th Ed. McMillan, New York.

Lloyd, R.M., 1968. Oxygen isotope behavior in the sulfate–water system. Journal of Geophysical Research Vol. 73 (18), 6099–6110.

Luther III, G.W., 1987. Pyrite oxidation and reduction: molecular orbital theory considerations. Geochimica et Cosmochimica Acta 51, 3193–3199.

Margalith, P., Silver, M., Lundgren, D.G., 1966. Sulfur oxidation by the iron bacterium *Ferrobacillus ferrooxidans*. Journal of Bacteriology 92 (6), 1706–1709.

Masau, R.J.Y., 1999. The mechanism of thiosulfate oxidation by *Thiobacillus thiooxidans*. Master Thesis. Faculty of Graduate Studies, Department of Microbiology, University of Manitoba, Winnipeg, Manitoba.158 p.

Macdonald, B.C.T., Denmead, O.T., White, I., Melville, M.D., 2004. Natural sulfur dioxide emissions from sulfuric soils. Atmospheric Environment 38, 1473–1480. doi:10.1016/j.atmosenv.2003.12.005.

Mielke, R.E., Pace, D.L., Porter, T., Southam, G., 2003. A critical stage in the formation of acid mine drainage: colonization of pyrite by *Acidithiobacillus ferrooxidans* under pH-neutral conditions. Geobiology 1 (1), 81–90. doi:10.1046/j.1472-4669.2003.00005.x.

Mustin, C., Berthelin, J., Marion, P., de Donato, P., 1992. Corrosion and electrochemical oxidation of a pyrite by *Thiobacillus ferrooxidans*. Applied and Environmental Microbiology 58 (4), 1175–1182.

Pisapia, C., Chaussidon, M., Mustin, C., Humbert, B., 2007. O and S isotopic composition of dissolved and attached oxidation products of pyrite by *Acidithiobacillus ferrooxidans*: comparison with abiotic oxidations. Geochimica et Cosmochimica Acta 71, 2474–2490. doi:10.1016/j.gca.2007.02.021.

Pronk, J.T., Meulenberg, R., Hazeu, W., Bos, P., Kuenen, J.G., 1990. Oxidation of reduced inorganic sulphur compounds by acidophilic thiobacilli. FEMS Microbiology Reviews 75, 293–306.

Ramírez, P., Guiliani, N., Valenzuela, L., Beard, S., Jerez, C.A., 2004. differential protein expression during growth of *Acidithiobacillus ferrooxidans* on ferrous iron, sulfur compounds, or metal sulfides. Applied and Environmental Microbiology 70 (8), 4491–4498. doi:10.1128/AEM.70.8.4491-4498.2004.

Rawlings, D.E., 2005. Characteristics and adaptability of iron- and sulfur-oxidizing microorganisms used for the recovery of metals from minerals and their concentrates. Microbial Cell Factories 4 (13), 1–15. doi:10.1186/1475-2859-4-13.

Rimstidt, J.D., Vaughan, D.J., 2003. Pyrite oxidation: a state-of-the-art assessment of the reaction mechanism. Geochimica et Cosmochimica Acta 67 (5), 873–880. doi:10.1016/S0016-7037(02)01165-1.

Rohwerder, T., Sand, W., 2003. The sulfane sulfur of persulfides is the actual substrate of the sulfur-oxidizing enzymes from *Acidithiobacillus* and *Acidiphilium* spp. Microbiology 149, 1699–1709. doi:10.1099/mic.0.26212-0.

Sand, W., 1989. Ferric iron reduction by *Thiobacillus ferrooxidans* at extremely low pH-values. Biogeochemistry 7, 195–201.

Schippers, A., Sand, W., 1999. Bacterial leaching of metal sulfides proceeds by two indirect mechanisms via thiosulfate or via polysulfides and sulfur. Applied and Environmental Micorbiology 65, 319–321.

Shortt, B.J., Darrach, M.R., Holland, P.M., Chutjian, A., 2005. Miniaturized system of a gas chromatograph coupled with a Paul ion trap mass spectrometer. Journal of Mass Spectrometry 40, 36–42.

Sugio, T., Hirose, T., Oto, A., Inagaki, K., Tano, T., 1990. the regulation of sulfur use by ferrous ion in *Thiobacillus ferrooxidans*. Agricultural and Biological Chemistry 54 (8), 2017–2022.

Sugio, T., Hirose, T., Li-Zhen, Y., Tano, T., 1992. Purification and some properties of sulfite: ferric ion oxidoreductase from *Thiobacillus ferrooxidans*. Journal of Bacteriology 174 (12), 4189–4192.

Sugio, T., Uemura, S., Makino, I., Iwahori, K., Tano, T., Blake II, R.C., 1994. Sensitivity of iron-oxidizing bacteria, *Thiobacillus ferrooxidans* and *Leptospirillum ferrooxidans*, to bisulfite ion. Applied and Environmental Microbiology 60 (2), 722–725.

Sugio, T., Hisazumi, T., Kanao, T., Kamimura, K., Takeuchi, F., Negishi, A., 2006. Existence of aa3-type ubiquinol oxidase as a terminal oxidase in sulfite of *Acidithiobacillus thiooxidans*. Bioscience, Biotechnology, and Biochemistry 70 (7), 1584–1591.

Suzuki, I., Chan, C.W., Takeuchi, T.L., 1992. Oxidation of elemental sulfur to sulfite by *Thiobacillus thiooxidans* cells. Applied and Environmental Microbiology 58 (11), 3767–3769.

Takeuchi, T.L., Suzuki, I., 1994. Effect of pH on sulfite oxidation by *Thiobacillus thiooxidans* cells with sulfurous acid or sulfur dioxide as a possible substrate. Journal of Bacteriology 176 (3), 913–916.

Taylor, B.E., Wheeler, M.C., Nordstrom, D.K., 1984. Stable isotope geochemistry of acid mine drainage: experimental oxidation of pyrite. Geochimica et Cosmochimica Acta 48, 2669–2678.

Toran, L., Harris, R., 1989. Interpretation of sulfur and oxygen isotopes in biological and abiological sulfide oxidation. Geochimica et Cosmochimica Acta 53, 2341–2348.

Turchyn, A.V., Schrag, D.P., 2006. Cenozoic evolution of the sulfur cycle: insight from oxygen isotopes in marine sulfate. Earth and Planetary Science Letters 241, 763–779. doi:10.1016/j.epsl.2005.11.007.

Uyama, F., Chiba, H., Kusakabe, M., Sakai, H., 1985. Sulfur isotope exchange reactions in the aqueous system: thiosulfate-sulfide-sulfate at hydrothermal temperature. Geochemical Journal 19, 301–315.

Vestal, J.R., Lundgren, D.G., 1971. The sulfite oxidase of *Thiobacillus ferrooxidans* (*Ferrobacillus ferrooxidans*). Canadian Journal of Biochemistry 49, 1125–1130.

Wakai, S., Kikumoto, M., Kanao, T., Kamimura, K., 2004. Involvement of sulfide:quinone oxidoreductase in sulfur oxidation of an acidophilic iron-oxidizing bacterium, *Acidithiobacillus ferrooxidans* NASF-1. Bioscience, Biotechnology, and Biochemistry 68 (12), 2519–2528.

Williamson, M.A., Rimstidt, J.D., 1993. The rate of decomposition of the ferric-thiosulfate complex in acidic aqueous solutions. Geochimica et Cosmochimica Acta 57, 3555–3561.

Wodara, C., Bardischewsky, F., Friedrich, C.G., 1997. Cloning and characterization of sulfite dehydrogenase, two c-type cytochromes, and a flavoprotein of *Paracoccus denitrificans* GB17: essential role of sulfite dehydrogenase in lithotrophic sulfur oxidation. Journal of Bacteriology 179 (16), 5014–5023.

Yarzábal, A., Appia-Ayme, C., Ratouchniak, J., Bonnefoy, V., 2004. Regulation of the expression of the *Acidithiobacillus ferrooxidans* rus operon encoding two cytochromes c, a cytochrome oxidase and rusticyanin. Microbiology 150, 2113–2123. doi:10.1099/mic.0.26966-0.

Yu, J.Y., McGenity, T.J., Coleman, M.L., 2001. Solution chemistry during the lag phase and exponential phase of pyrite oxidation by *Thiobacillus ferrooxidans*. Chemical Geology 175, 307–317.

Zak, I., Sakai, H., Kaplan, I.R., 1980. Factors controlling the $^{18}O/^{16}O$ and $^{34}S/^{32}s$ isotope ratios of ocean sulfates, evaporites and interstitial sulfates from modern deep sea sediments. Isotope Marine Chemistry, Chapter 17. Institute of Geophysics and Planetary Physics, University of California Los Angeles, California 90024, USA, pp. 339–373. Contribution No. 1957.